



Optimised Cross-Spring Pivot Configurations with Minimised Parasitic Shifts and Stiffness Variations Investigated via Nonlinear FEA

Kristina Marković & Saša Zelenika

To cite this article: Kristina Marković & Saša Zelenika (2016): Optimised Cross-Spring Pivot Configurations with Minimised Parasitic Shifts and Stiffness Variations Investigated via Nonlinear FEA, *Mechanics Based Design of Structures and Machines*, DOI: [10.1080/15397734.2016.1231614](https://doi.org/10.1080/15397734.2016.1231614)

To link to this article: <http://dx.doi.org/10.1080/15397734.2016.1231614>



Accepted author version posted online: 03 Sep 2016.
Published online: 03 Sep 2016.



Submit your article to this journal [↗](#)



View related articles [↗](#)



View Crossmark data [↗](#)

Optimised Cross-spring Pivot Configurations with Minimised Parasitic Shifts and Stiffness Variations Investigated Via Nonlinear FEA

Kristina Marković

Faculty of Engineering, University of Rijeka, Rijeka, Croatia

Centre for Micro- and Nano-Sciences and Technologies, University of Rijeka, Rijeka, Croatia

Saša Zelenika

Faculty of Engineering, University of Rijeka, Rijeka, Croatia

Centre for Micro- and Nano-Sciences and Technologies, University of Rijeka, Rijeka, Croatia

Address correspondence to Kristina Marković.

Abstract

Compliant mechanisms are nowadays a well-established means of achieving ultra-high precision, albeit at the expense of complex kinematics with the presence of parasitic motions. Diverse design configurations of compliant rotational joints called cross-spring pivots are hence studied in this work by applying various analytical and numerical approaches. Depending on the required precision and loading conditions, the limits of applicability of the available analysis tools, validated with nonlinear finite element calculations tuned with experimental data reported in literature, are established. The variation of design parameters allows, in turn, establishing design configurations of the studied mechanism that allow attaining minimised parasitic shifts and slight variations of its rotational stiffness, even when a broad range of rotations and varying transversal loads are considered, creating thus the preconditions for their application in high-precision micropositioning applications.

Keywords: compliant mechanisms, cross-spring pivot, high-precision positioning, nonlinear FEA modelling, optimised design configurations

1. INTRODUCTION

When transfer of motion, energy and power is to be accomplished, compliant mechanisms are a valid alternative to sliding and rolling mechanisms, especially in precision engineering and microsystem technologies, i.e. when achieving high-precision positioning can be far more important than the motion range or the load capacity of the mechanism itself. In fact, since compliant mechanisms gain at least part of their mobility from the deflection of flexible members, often in the form of spring-strips, they are characterised by the absence of friction, backlash and wear, limited hysteresis, reduced costs as well as the possibility of monolithic manufacturing and thus of “design-for-no-assembly”. The resulting main error sources are hence systematic and high precision, accuracy and resolutions can therefore be obtained even when relatively simple control laws are used. Owing to these advantages, in addition to the mentioned technological fields, compliant mechanisms are thus widely used also in mechanical engineering design, metrology and scientific instrumentation, information & communications technology (ICT), aerospace and astrophysics, machine tools, robotics or biomedical applications (National Physical Laboratory 1956; Jones 1962; Smith and Chetwynd 1992; Smith 2000; Yin and Ananthasuresh 2003; De Bona and Zelenika 2006; Howell 2010; Pavlović and Pavlović 2013; Bhattacharya, Bepari, and Bhaumik 2014; Ivanov and Corves 2014; Khan and Ananthasuresh 2014).

The design arrangement of a compliant rotational joint obtained, as shown in **Figure 1**, by using spring-strips, is often referred to as the cross-spring pivot. It is characterised by a marked compliance along the ‘in plane’ rotational degree of freedom and high stiffness (order of

magnitudes higher than that along the main degree of freedom) along the secondary (transversal) degrees of freedom.

As shown in **Figure 2**, cross-spring pivots consist of a rigid body B connected by using spring-strips 1 and 2, generally crossing at their midpoints, with a movable block A. In the usual configuration, the used spring-strips have the same length L , width b and thickness t (**Figure 2a**) and are made of the same spring material with a high figure of merit given by the yield strength – to – Young 's modulus ratio σ_y/E .

In the general case habitually considered in literature and mostly used in practical applications, the cross-spring pivot is loaded with a pure couple M , thus allowing the movable block A to rotate, via the deflection of the spring-strips, with respect to fixation B (**Figure 2b**). For larger rotation angles θ , however, the ‘geometrical’ centre of the pivot O moves to point O’, defined by the tangents to the fixed ends of the strips in the movable block, giving hence rise to a parasitic shift of amplitude d and phase φ . This parasitic motion is, obviously, detrimental to the precision of the analysed mechanisms. What is more, when loaded with transversal forces H and V (also shown in **Figure 2b**) that can also appear in some practical applications, the range of stability of the mechanism can be limited, since buckling can occur in one or both spring-strips, hence inducing a negative restoring moment for the whole mechanism, i.e. the occurrence of its negative rotational stiffness (Wittrick 1948; Haringx 1949; Siddall 1970; Zelenika and De Bona 2002).

In order to assess the influence of these harmful effects on the performances of cross-spring pivots, the equilibrium of loads and internal reactions of the whole mechanism (**Figure 2b**) has to be considered. This can be brought down to the analysis of the stress-strain behaviour, i.e. the equilibrium of forces and torques acting on the single spring-strips. In this frame, only the planar

behaviour of the strips is considered since, due to their thickness – to – width ratio t/b and the respective values of the second moments of area, their secondary compliances, as already pointed out, are orders of magnitude smaller, and thus less relevant, than the main bending compliance (cf. in this regard Lobontiu 2003; Henein 2001). Several analytical and experimental approaches have been used so far in literature to study this problem (Young 1944; Wittrick 1948; Haringx 1949; Wuest 1950; Nickols and Wunsch 1951; Hildebrand 1958; Troeger 1962; Siddall 1970; De Bona and Zelenika 1993; De Bona and Zelenika 1997; Jensen and Howell 2002; Zelenika and De Bona 2002; Pei et al. 2010).

The aim of this work is to establish the limits of applicability of the diverse modelling approaches available in literature for the analysis of the behaviour of cross-spring pivots depending on the required accuracy and precision. The work aims also at determining optimised design configurations of the pivot that allow minimising the parasitic shifts and the variability of rotational stiffness, while preserving the stability of the mechanism, its simple design and its reliability.

In section 2 of the paper, a nonlinear finite element model (FEM) of the cross-spring pivot, validated by comparing the thus obtained results with experimental measurements available in literature, is hence developed by using the ANSYS® FEM software package. This numeric model is then used in section 3 to assess the accuracy limits of the modelling approaches used so far in literature to model the behaviour of symmetrical cross-spring pivots loaded by a pure couple.

By employing the same structured FEM calculation procedure, variants of the design of the pivot, where the angle, the point of crossing or the initial curvature of the springs are modified, or, alternatively, the midpoint of the springs is joined in a monolithic (“cartwheel”) design configuration, or a symmetrical compound “butterfly” design configuration of the pivot is used, are all analysed in section 4. Design solutions that minimise the parasitic shifts while guaranteeing

the stability of the mechanism and a minimal variability of its rotational stiffness, even in the presence of lateral loads, are hence identified. These design configurations create the preconditions for a new class of micropositioning high-precision compliant rotational joints.

2. NONLINEAR NUMERICAL MODEL

In prior art it has been established that the analysis of the behaviour of cross-spring pivots for high-precision applications, including the parasitic shifts of their geometrical centre, involves the modelling of large (geometrically nonlinear) deflections of the spring-strips (Haringx 1949; De Bona and Zelenika 1997; Zelenika and De Bona 2002). By using the ANSYS® FEM package, the kinematics of the cross-spring pivots is hence modelled numerically in this work via a nonlinear large deflection finite element analysis (FEA). BEAM189 quadratic 3D three-node elements with six degrees of freedom at each node, based on Timoshenko's modification of the conventional Euler-Bernoulli beam theory (Ansys 2014), are used. An idealization of the three-dimensional cross-spring pivot structure with not-intersecting leaf springs A_1B_1 and A_2B_2 (**Figure 3a**), whose fixations B_1 and B_2 have all the degrees of freedom (DOFs) constrained (**Figure 3b**), is thus created. The chosen elements support nonlinear analyses including geometrically nonlinear deflections. The undeformable rigid movable body is, in turn, modelled by imposing the value of its stiffness (i.e. its Young's modulus) by orders of magnitude higher than that of the leaf springs. The calculation is hence performed so that the maximum foreseen rotation of the cross-spring pivot is divided in 10 equal sub-steps. In each sub-step the iterative pursuit of a stable solution is continued until the convergence criteria is satisfied, while the maximum number of allowed iterations is set to 50. Convergence tests proved that with 1 mm long BEAM189 elements, convergence is always obtained.

To take into account also the influence of the anticlastic effect, that induces a transversal stiffening of the spring-strips that is nonlinearly proportional to their deflection (Ashwell 1950; Angeli et al. 2006; Hao et al. 2016), the input parameters for the FEM calculations are, moreover, modified so that, depending on the deflection, the nominal value of Young's modulus E is changed towards $E/(1-\nu^2) = \Phi E$, where ν is Poisson's ratio of the spring-strip material, whereas Φ is a corrective factor for the value of Young's modulus. In fact, for a given rotation θ of the pivot and the corresponding leaf spring curvature $1/r$, with springs having a thickness – to – width ratio t/b , E will change towards $E/(1-\nu^2)$ according to the curves depicted in **Figure 4**. For a given θ , the deflection of the leaf spring is thus calculated by using the nonlinear FEA model where the relevant mechanical parameter is assumed to Young's modulus E . Depending on the dimensions of the leaf springs and the obtained curvature in the deformed position, the value of the factor Φ is hence determined from the relevant curve in **Figure 4**. This factor is used to modify the value of E in the input parameters for the next iteration of the FEA calculation. The procedure is repeated until in subsequent calculation steps the value of Φ does not change more than 0.01%, which is generally achieved in maximally 2-3 iterations.

The thus developed FEA model allows, hence, the amplitude d and the phase φ of the parasitic shifts of the geometrical centre of the pivot in its deformed position to be determined. This is achieved by monitoring the dependence of the motion of the free end of a thin stiff beam $\overline{OA_3}$ vs. the rotation θ of pivot's movable block A towards its final position A' (see **Figures 3b & 3c**). The dimensions and the characteristics of the material of the spring-strips used in the FEA model are those considered in the most recent experimental measurements reported in (Zelenika and De Bona 2002), i.e. the spring-strips' length, width and thickness are, respectively, $L = 115$ mm, $b = 15$ mm and $t = 0.5$ mm, the angle between the spring-strips is $2\alpha = 90^\circ$, whereas the modulus of

elasticity and Poisson's ratio of the beryllium-copper spring-strips are, respectively, $E = 1.31 \cdot 10^{11}$ Pa and $\nu = 0.285$. This implies that the overall number of elements in the FEA model is limited to 350.

In order to assess the applicability of the thus arranged numerical model in predicting the stress-strain behaviour of the considered class of mechanisms, the results obtained by using the FEA model and thus compared with the results of experimental measurements reported in literature for the most common case of pivots loaded with a pure couple M (Young 1944; Wuest 1950; Nickols and Wunsch 1951; Hildebrand 1958; Siddall 1970; Zelenika and De Bona 2002). The comparison, shown in **Figure 5**, is performed, in a first instance, in terms of the normalized parasitic shift amplitudes d/L versus pivots' rotation θ . The exponentially growing values of d/L obtained via the FEA model, shown as the dot-dashed line, can hence be read on the left ordinate in **Figure 5**. In order to enhance the visibility of the data, depicted in the figure (with values referred to the secondary vertical axis) are the differences $\Delta d/L$ of the experimental results given in literature with respect to these FEA values. It can thus be seen that, although the measurement techniques used in most of prior art allow the general trends of the parasitic shifts' magnitudes to be well identified, they are generally characterized by high uncertainties and are thus not so relevant. In fact, the results attained by Siddall (1970 – dashed line with cross markers in **Figure 5**), Wuest (1950 – dashed compound line), Hildebrand (1958 – dotted line with triangular markers), Nickols and Wunsch (1951 – dashed line with circular markers) and Young (1944 – solid line), were obtained by using contact or low-resolution non-contact measurement techniques based on styluses, pointers or measuring and toolmakers' microscopes. Only the results of recently performed experimental measurements based on a Michelson-type laser Doppler interferometric system (solid compound line with error bars in **Figure 5**), are characterised by high accuracies and

small intervals of uncertainty (Zelenika and De Bona 2002). In **Figure 5** it is evident that these results match excellently the FEA results. In fact, in the whole considered large range of pivot rotations ($0 < \theta \leq 30^\circ$), the differences between the interferometric measurements and the results of FEM analyses are smaller than 2% (i.e. for d/L calculated by using FEM analysis ≈ 0.03 , the resulting deviation $\Delta d/L$ of the interferometric measurements is ≈ 0.0005). These residual deviations could be due to errors induced in the mounting procedure used in the considered measurement set-up as well as the compliance of the fixation of the spring-strips themselves.

FEA results obtained for parasitic shifts' phases φ , as well as for the rotational stiffness of the pivot, are also matching well the experimental measurement results. In fact, in **Figure 6** are compared the results in term of rotational stiffness obtained by using FEM analysis (dot-dashed line) with one of the very few relevant experimental results available in literature for this parameter – those reported by Young (1944 – solid line). It can be seen that the two lines are very adjacent to each other. All this confirms, therefore, that the arranged FEA calculation procedure is a computationally efficient and accurate tool for the prediction of the behaviour of cross-spring pivots. This hence creates the preconditions for using the FEA model in validating the analysis tools proposed so far for the study of the behaviour of the considered class of mechanisms, as well as to study the influence of the design parameters on their behaviour, thus optimising the resulting design configurations.

3. VALIDATION OF THE LIMITS OF APPLICABILITY OF ANALYTICAL AND NUMERICAL METHODS PROPOSED IN LITERATURE

The structured and verified FEA model developed in the ANSYS® software package is used next to assess, depending on the required degrees of accuracy, the limits of applicability of the analytical and numerical methods proposed in literature for modelling the behaviour of generally used symmetrical cross-spring pivots loaded with a pure couple M (Wittrick 1948; Haringx 1949; Wuest 1950; Troeger 1962; De Bona and Zelenika 1993; De Bona and Zelenika 1997; Jensen and Howell 2002; Zelenika and De Bona 2002; Pei et al. 2010). The results obtained via the FEA numerical method in the frame of this work are thus compared with those obtained by using:

- The Elastica approach (EL) that takes into account the exact expression for the curvature of the spring-strips in the domain of large (geometrically nonlinear) deflections, i.e. where the stress-strain relationship is influenced by the value of the deflection of the strip itself (Haringx 1949; De Bona and Zelenika 1997).
- Approaches based on approximated expression for the curvature of the beam where the influence of the axial components of the load on spring-strips' bending is still considered, but the square of the derivative in the curvature formula is neglected (Wittrick 1948; AC – Zelenika and De Bona 2002).
- Approaches based on the pseudo-rigid-body model (PRBM), where an equivalent mechanism, constituted by rigid members hinged via suitably positioned pinned rotational joints comprising torsional springs, so as to generate the same load-displacement characteristic as the original mechanisms (in this case cross-spring pivot), is studied. In particular, in this work are considered PRBM cross-spring pivot configurations optimised in literature via lengthy FEM calculations, i.e. the 'pin joint' (**Figure 7a**) and the 'four bar' arrangements (**Figure 7b**) analysed in (Jensen and Howell 2002), as well as the

configuration where each spring-strip is substituted with a rigid bar with two pin joints but, as proposed in (Pei et al. 2010), only one of these is coupled with a torsional spring of equivalent stiffness (**Figure 7c**).

- Approaches based on a kinematic model (KM) of the cross-spring pivot (Wuest 1950).
- Geometrical methods (GM) as proposed in (Troeger 1962) or those based on a simple hinged frame with four rigid bars as suggested in (De Bona and Zelenika 1993).

The comparison of the results obtained with the cited approaches is reported in **Figure 8a** in terms of the exponential rise of the normalised parasitic shift amplitudes d/L , and in **Figure 8b** in terms of the couple M needed to achieve the rotation of the cross-spring pivot for a given rotation angle θ (which, in turn, correlates linearly with the rotational stiffness of the pivot). The comparison of the results is, once more, easier if the differences $\Delta d/L$ and ΔM of the results obtained with the various considered approaches with respect to the FEM values, achieved by using the model of section 2, are reported (secondary vertical axes in **Figure 8**). The respectively reported data should thus be considered bearing in mind the extensive explanation given in relation to **Figure 5**.

From the curves depicted in **Figure 8a** it can hence be observed that the EL results of the parasitic shift amplitudes (dashed line with rectangular markers in the figure), which take into account the nonlinear effects, practically coincide with FEM analysis results even for large rotation angles of the pivot. The EL approach is, however, computationally intensive due to the presence of elliptic integrals that have to be iteratively evaluated in the calculation routine (De Bona and Zelenika 1997).

Amongst the approximate analytical methods, the ‘two pin joints’ PRBM approach (Pei et al. 2010 – solid line with circular markers in **Figure 8a**) results in the smallest deviations. The AC

(dashed line), KM (dotted line with filled rhomboidal markers) and GM (compound line with filled circular markers) approaches suggested, respectively, in (Zelenika and De Bona 2002), (Wuest 1950) and (Troeger 1962), are in good agreement with FEA results for rotation angles θ smaller than 15° , while the errors exponentially increase for larger rotations. Finally, the PRBM results obtained by using the approaches proposed in (Jensen and Howell 2002 – compound line with rhomboidal markers and dotted line in **Figure 8a**), as well as the GM results according to (De Bona and Zelenika 1993 – compound line), allow only a first-degree approximation of the real behaviour of cross-spring pivots loaded with a pure couple and can thus be used merely in the initial design phases when the early design concepts are quickly screened.

When the phase φ of the parasitic shift is considered (not shown in the **Figure 8** for clarity reasons), it is established that, in agreement with FEA results, the EL model of (Haringx 1949), the GM approaches suggested in (Troeger 1962) and (De Bona and Zelenika 1993) and the four bar PRBM approach of (Jensen and Howell 2002), all allow establishing that $\varphi = \theta/2$, while the KM approach of (Wuest 1950) underestimates the value of φ , whereas the results obtained by using the PRBM pin joint approach (Pei et al. 2010) lead to an overestimate of these values.

On the other hand, from the comparison of the couples needed to induce a determined rotation θ of the cross-spring pivot, depicted in **Figure 8b** (with line types used for the various available methods coinciding with those of **Figure 8a**), it can be established that the EL results are again coinciding with FEA results in the whole considered range of rotations. The results obtained by employing the AC approach suggested in (Wittrick 1948) produce errors that markedly increase for increasing rotation angles θ , whereas the four bar PRBM approach (Jensen and Howell 2002) gives relatively good results (within $\pm 1\%$) for rotation angles θ larger than 10° . Results obtained by using the PRBM pin joint arrangement (Jensen and Howell 2002 – that in this case are equal

with those obtainable with the two pin joint PRBM approach proposed in (Pei et al. 2010)), produce considerable errors, while the other considered modelling approaches do not allow the value of the couple M to be calculated.

Considering, finally, the maximal stresses that occur in the cross-spring pivot, it is concluded that, for rotation angles θ limited to 30° , these reach barely 180 MPa and are thus much lower than the yield strength of the considered beryllium copper material ($\sigma_y = 1124$ MPa). The EL approach (Haringx 1949) provides once more results corresponding to those obtained by employing the FEA nonlinear calculation, whereas the four bar PRBM (Jensen and Howell 2002) produces errors of up to 5% that decrease with increasing rotation angles.

Based on these consideration, it can be concluded that only the EL approach allows reliable results to be obtained, albeit at the expense of considerable computational intensity. The approximate analysis tools suggested in prior art can be used only in limited ranges of rotations of the cross-spring pivot and, depending on the performance parameters related to the behaviour of the pivot that are monitored, these ranges may even not always coincide. When an accurate model of the overall behaviour of the cross-spring pivots is needed, which is generally anyway the case in all high-precision micropositioning applications, a nonlinear FEA model of the device will thus have to be preferred.

4. STUDY OF THE INFLUENCE OF DESIGN PARAMETERS

Based on the above treatise, the established nonlinear FEM calculation procedure is used next to study the effects induced by the variation of design parameters on the minimisation of the parasitic shifts and of the variability of the rotational stiffness for diverse design configurations of cross-spring pivots. In this work are hence systematically considered the variations of:

- the angle α defining the inclination of the spring-strips with respect to the vertical axis of the cross-spring pivot (**Figure 9a**);
- the longitudinal position of crossing of the spring-strips defined by the geometric parameter λ (**Figure 9a**);
- the initial curvature of spring-strips defined by the angles γ_1 and γ_2 at their fixations in, respectively, the fixed and the movable block (**Figure 9b**); as well as design configurations where:
- the spring-strips are joined in pivots' geometrical centre O so as to create a monolithic (“cartwheel”) configuration of the mechanisms (**Figure 9c**);
- a compound “butterfly” design configuration of the pivot (basically constituted by two interlayered cross-spring pivots with an intermediate movable block C) is used (**Figure 9d**);
- and additional external transversal loads (H and V in **Figure 2b**) are applied to the pivot.

4.1. Influence of Spring-strips' Inclination α on the Performances of Cross-spring Pivots

Results regarding the performances of cross-spring pivots obtained via the nonlinear FEM analyses allow establishing that, for a determined inclination angle α of the spring-strips, the values of the normalised parasitic shift amplitudes d/L do not change when the geometric parameters of the strips (i.e. L , b and t of **Figure 2a**) are varied. On the other hand, as visible in **Figure 10a**, an increase of the value of α results in a rise of the value of d/L that is more pronounced for larger rotations θ of the pivot. A variation of α does not have an influence on the value of the parasitic shift phases φ (i.e. the value of the phase remains $\varphi = \theta/2$ irrespective of the value of α).

An increase of the value of the inclination angle α results also in a marked increase of the normalised rotational stiffness $KL/(EI)$ of the pivot (with $K = M/\theta$ – **Figure 10b**) and in an almost linear increase of the stresses σ_{\max} in the fixations of the spring-strips (normalised here with respect to the yield strength of the considered beryllium copper strips' material – **Figure 10c**).

4.2. Influence of the Geometric Parameter λ on the Performances of Cross-spring Pivots

When in the nonlinear FEM calculation procedure, for a fixed inclination $\alpha = 45^\circ$ of the spring-strips, a variation of the position of the geometrical centre O of the pivot along spring-strips' length, defined via the parameter λ of **Figure 9a**, is imposed, results shown in **Figure 11** are obtained. It is thus evident that the variation of λ induces a substantial variation of the normalised parasitic shift amplitudes d/L (**Figure 11a**); the phase φ of the parasitic shifts (not shown graphically) is, in turn, maximal when d/L tends to minimal values, i.e. in these cases the parasitic shift is almost horizontal. The variation of λ causes also a considerable change of the normalised rotational stiffness (**Figure 11b**) and of the normalised stresses at the fixed ends of the spring-strips (**Figure 11c**).

It is important to note here especially that, for a design configuration for which the geometric parameters are, respectively $\alpha = 45^\circ$ and $\lambda \approx 0.13$ (which is, obviously, mechanically equivalent to the mirrored configuration with $\lambda \approx 0.87$), the parasitic shifts become negligible even for large rotation angles θ , at the expense, however, of a conspicuous increase of rotational stiffness and the stresses. Contrary to what is generally reported in literature where, basing the studies of the overall behaviour of the pivot mostly on the approximated expression for the curvature of the beam considered in section 3 (i.e. on small pivot rotations), it is stated that the

value of the parameter λ that allows minimising the parasitic shifts is constant (Wittrick 1951; Hongzhe and Shusheng 2010; Pei et al. 2010; Goncalves et al. 2014), the nonlinear FEM analyses allow establishing that the value of λ that allows minimising the parasitic shifts will change depending on the inclination α of the spring-strips and on the magnitude of pivot's rotation θ . For $\alpha = 15^\circ$ the minimal parasitic shifts will hence be obtained for a rotation of $\theta = 5^\circ$ when $\lambda = 0.127$, and for a rotation of $\theta = 30^\circ$ when $\lambda = 0.175$. On the other hand, in the case when $\alpha = 30^\circ$ and the rotation of the pivot is varied between $5^\circ \leq \theta \leq 30^\circ$, the parasitic shifts will be minimised for values of the geometric parameter λ in the range of, respectively, $0.127 \leq \lambda \leq 0.133$, whereas, for the same range of pivot rotations, in the case with $\alpha = 45^\circ$, the value of the shifts will be minimal for $0.127 \leq \lambda \leq 0.1305$.

4.3. Influence of Spring-strips' Initial Curvature on the Performances of Cross-spring Pivots

The systematic nonlinear numerical analysis of cross-spring pivot configurations with an initial curvature of the spring-strips (**Figure 9b**), which can be the result of the rolling process often used in the manufacturing of thin sheets of alloys aimed at leaf springs, and has been suggested as a possible design configuration in a very specific case considered in (Hildebrand 1958), allows establishing that this configuration induces significantly larger parasitic shifts than the conventional pivots' configurations of **Figure 2**, accompanied by a large increase of rotational stiffness and of the stresses. In fact, even the configuration with a combination of spring-strips' inclinations $\gamma_1 = 15^\circ$ and $\gamma_2 = 60^\circ$, that results in the smallest parasitic shift amplitudes, gives still rise to values of the parasitic shifts, of the stiffness and of the stresses markedly larger than those

obtained in the case of design configurations with straight spring-strips analysed so far. It can thus be concluded that the initial curvature of the spring-strips should, if possible, be avoided.

4.4. Performances of a Monolithic Configuration of the Cross-spring Pivot

When compared to a conventional pivot's configuration of **Figure 2**, a monolithic configuration of the cross-spring pivot shown in **Figure 9c** where, as suggested in (Pei et al. 2010), the spring-strips are joined in the geometrical centre O of the pivot, and considering variable spring-strips' inclination angles α , whereas $l_1 = l_2 = L/2$, analysed again via nonlinear FEM models, leads to a decrease of parasitic shifts of up to even 8 times (!). This is achieved, however, at the expense of a conspicuous increases of pivot's stiffness and of the stresses induced in the spring-strips (by roughly up to four times) – see **Figure 12**. On the other hand, the variability of the stiffness and the stresses in the considered range of rotations is rather small, while, regarding the phase of the parasitic shifts, the relation $\varphi = \theta/2$ is still valid.

4.5 Performances of a “Butterfly” Design Configuration of the Cross-spring Pivot

In order to minimise the parasitic shifts of compliant mechanisms based on spring-strips aimed at linear motions, while increasing their motion range, symmetrical compound devices, first proposed by Jones (1962) and recently elaborated both theoretically and experimentally in far more detail (De Bona and Zelenika 1993; Hao and Li 2016; Hao and Yu 2016), have been proposed. The same concept for achieving a planar rotational motion is that of a “butterfly” pivot shown in **Figure 9d**, suggested in literature for an application in a scanning device for space instrumentation (i.e. inter-satellites communication systems – Henein et al. 2003). When the rotation of this complex and technologically rather cumbersome monolithic cross-spring pivot is analysed by employing nonlinear FEA configured in the ANSYS® software package, results shown in **Figure**

13 are obtained. In this case the values of the parasitic shift amplitudes (**Figure 13a**) decrease further by roughly up to four times with respect to those of the cartwheel monolithic pivot configuration of section 4.4, whereas the increase of the stresses with respect to the conventional pivot configuration is considerably mitigated, so that the maximal stresses shown in **Figure 13b** are roughly two times larger than those obtained in the case of the most common pivot configuration of **Figure 2**. The “butterfly” pivot configuration allows, hence, a large span of rotations to be covered with small parasitic shifts, albeit at the expense of technological difficulties in manufacturing and mounting the pivot, which can considerably influence the resulting costs.

4.6. Influence of Transversal Loads on the Performances of Cross-spring

Pivots

In the above study, the case of pivots loaded only with a pure couple M was considered. In this section, the nonlinear FEM analysis is extended also to the study of the influence of external transversal loads on the variability of rotational stiffness and on the entity of the parasitic shifts. In fact, in prior art (Wittrick 1951; Zelenika and De Bona 2002; Hongzhe and Shusheng 2010; Goncalves et al. 2014), despite the limited accuracy of the used simulation tools (cf. section 3), it was shown that these loads, which are occasionally present in practical applications of cross-spring pivots, can have a significant influence on the behaviour of the considered class of mechanisms, especially when the geometric parameter λ is varied as well.

Physically, the influence of a horizontal transversal force H can be seen as a mere superposition to the effect of the couple M . In **Figure 14** are therefore shown the results of nonlinear numerical analyses of the influence of the vertical external load V (acting concurrently with M and loading the pivot in tension or in compression) on the normalized rotational stiffness $KL/(EI)$ of the cross-spring pivots when the angle of inclination of the spring-strips is $\alpha = 45^\circ$.

It can thus be seen that the vertical external load has indeed a big influence on the performances of cross-spring pivots. In fact, when a compressive vertical force V_C loads the pivot, its stability range (i.e. the range where rotational stiffness is positive) is substantially narrowed. When compared to the performances of the most common pivot's configuration loaded with a pure couple, this loading condition induces, in fact, also an increase of rotational stiffness, an increase of the stresses in the spring-strips and a decrease of parasitic shift amplitudes. By lowering the value of the angle of inclination of the spring-strips α (i.e. considering $\alpha = 30^\circ$ or even $\alpha = 15^\circ$), the range of values of compressive external load V_C for which the rotational stiffness of the pivot is positive is, however, extended. On the other hand, a tensile external load V_T can induce again an increase of the stresses, but also a decrease of rotational stiffness as well as an increase of parasitic shift amplitudes.

Tensile external loads, with a concomitant variation of the position λ of crossing of the spring-strips along their lengths, induce then a broadening of the stability range of the pivots (that where rotational stiffness is positive). As visible in **Figure 14** (cf. especially the upper zoomed region in the figure), the cross-spring pivot configuration with $\lambda = 0.1$, loaded with a tensile external force, allows hence achieving a slight variation of rotational stiffness and small parasitic shifts for the whole range of vertical tensile loads where $V_T L^2 / (EI) \leq 30$. On the other hand, design configuration for which the geometry of the pivot is such that $\lambda \approx 0.13$ (i.e. the one for which, as shown in **Figure 11**, the parasitic shift amplitudes are negligible), permits, in turn, accomplishing a very small variation of rotational stiffness as long as $|V L^2 / (EI)| \leq 10$, i.e. irrespective of the orientation of vertical loads – see lower zoomed region of **Figure 14**.

Design configurations that allow minimising the parasitic shift amplitudes, while guaranteeing a negligible variation of rotational stiffness and preserving the stability of the mechanism, are thus successfully determined.

5. CONCLUSIONS

Results obtained via suitably arranged nonlinear FEA models are compared in this work to experimental data on the behaviour of cross-spring pivots aimed at micropositioning applications, confirming their validity in a broad range of pivot rotations, i.e. even when large deflections of the spring-strips, implying the presence of geometrical nonlinearities, have to be considered. Numerical FEA is hence used to determine the range of applicability of the simulation models proposed in literature to study the behaviour of the considered class of mechanisms, allowing to establish that, in the case of pivots loaded merely with a pure couple, only the nonlinear and computationally demanding Elastica approach is suitable to model the behaviour of the pivots when high precisions and/or large rotation angles are aimed for, whereas the approximate analysis tools can be used only in limited ranges of pivots' rotations.

Nonlinear FEM, which allows to attain quick, accurate and reliable results, is subsequently used also to study thoroughly the influence of design parameters (various geometric and loading conditions) on the minimization of parasitic shifts and of the variability of the stiffness of the studied class of mechanisms. It is hence established that an optimal design configuration will always depend on the foreseen application of the pivot, i.e. it will be based on a compromise between configurations that allow improving some characteristic parameters of the pivots, while deteriorating, at least to some extent, some of the other parameters. The monolithic configuration of the cross-spring pivot allows, for example, to decrease substantially the parasitic shifts of the geometrical centre of the pivots, but at the expense of a concurrent increase of its stiffness and the

resulting stresses in the spring-strips, which could, in the case of larger rotation spans, endanger the structural integrity of the considered mechanisms. The symmetrical compound “butterfly” configuration allows attaining even smaller parasitic shifts with somewhat smaller stress levels, but its production is considerably more complex and thus costly.

A practically easily achievable design arrangement of the cross-spring pivot with the value of the geometric parameter $\lambda \approx 0.13$ allows, however, ultra-high precisions to be attained, as it is characterized by negligible parasitic shifts even for large pivot rotations, while concurrently guaranteeing also the stability of the mechanism and allowing to maintain the stress levels in the spring-strips well within the allowable limits. The values of the parameter λ that allow minimising parasitic shifts will, in turn, depend on spring-strips' inclination α , on the range of rotations θ , as well as on the transversal forces loading the pivot. In fact, pivot's configuration with $\lambda \approx 0.13$ and $\alpha = 45^\circ$ is characterized not only by small parasitic shifts, but also by a very limited variation of rotational stiffness as long as the transversal loads, acting on the pivot alongside the pure couple, are of limited value. For crossing points close to one of the pivots' blocks (i.e. for values $\lambda < 0.5$), vertical tensile forces loading the pivot seem to have, in turn, a positive effect on its stability. Stable pivot configurations with $\lambda = 0.1$ allow hence achieving small rotational stiffness variations and small parasitic shifts for a rather large span of tensile vertical loads.

It can thus be concluded that simple and reliable cross-spring pivot design configurations with the values of the geometric parameter λ in the $0.1 \leq \lambda \leq 0.13$ range could be applied in a broad range of ultra-high precision micropositioning applications such as, for instance, in the field of production or of handling and assembly of micro-electro-mechanical systems (MEMS).

Acknowledgements

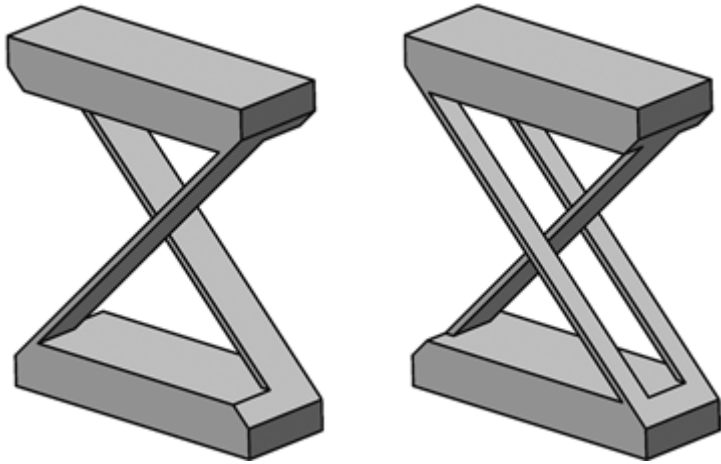
The work presented in this paper was partially supported by the University of Rijeka research grant no. 13.09.1.2.09. entitled “Characterisation and Modelling of Materials and Devices for Innovative Applications”.

References

- Angeli, P., F. De Bona, and M. Gh, and I. Civile. 2006. Micromeccanismi con molle a lamina: Valutazione della rigidezza flessionale. In Proc AIAS, Ancona.
- Anslys Inc. 2014. ANSYS 13.0 mechanical APDL.
- Ashwell, D. G. 1950. The anticlastic curvature of rectangular beams and plates. *Journal of the Royal Aeronautical Society* 54:708–15.
- Bhattacharya, S., B. Bepari, and S. Bhaumik. 2014. IPMC-actuated compliant mechanism-based multifunctional multifinger microgripper. *Mechanics Based Design of Structures and Machines* 42 (3):312–25. doi:10.1080/15397734.2014.899912
- De Bona, F., and S. Zelenika. 1993. Characterization of high precision parallel spring translators. In *International progress in precision engineering*, ed. N. Ikawa, S. Shimada, T. Moriwaki, P. A. McKeown, and R. C. Spragg, 761–72. Boston: Butterworth-Heinemann.
- De Bona, F., and S. Zelenika. 1997. A generalized elastica-type approach to the analysis of large displacements of spring-strips. *Proceedings of the Institution of Mechanical Engineers, Part C: Journal of Mechanical Engineering Science* 211 (7):509–17. doi:10.1243/0954406971521890
- De Bona, F., and S. Zelenika. 2006. Design of compliant micromechanisms. In *Microsystems mechanical design*, ed. F. De Bona and E. T. Enikov, 119–34. Wien & New York: Springer.
- Goncalves, Jr., L. A., Bitencourt, A. C. P., Theska, R., and Lepikson, H. A. 2014. Characterization of the elasto-kinematic behavior of generalized cross-spring bearings. In Proc 58th Ilmenau scientific colloquium, Ilmenau.
- Hao, G., and H. Li. 2016. Extended static modelling and analysis of compliant compound parallelogram mechanisms considering the initial internal axial force. *Journal of Mechanisms and Robotics* 8 (4):041008. doi:10.1115/1.4032592
- Hao, G., H. Li, S. Kemalcan, G. Chen, and J. Yu. 2016. Understanding coupled factors that affect the modelling accuracy of typical planar compliant mechanisms. *Frontier of Mechanical Engineering* 11 (2):129–34. doi:10.1007/s11465-016-0392-z
- Hao, G., and J. Yu. 2016. Design, modelling and analysis of a completely-decoupled XY compliant parallel manipulator. *Mechanism and Machine Theory* 102:179–95. doi:10.1016/j.mechmachtheory.2016.04.006
- Haringx, J. A. 1949. The cross-spring pivot as a constructional element. *Flow, Turbulence and Combustion* 1:313–32. doi:10.1007/BF02120338
- Henein, S. (2003). *Conception des guidages flexibles*. Lausanne: Presses polytechniques et universitaires romandes.
- Henein, S., P. Spanoudakis, S. Droz, L. I. Myklebust, and E. Onillon. 2003. Flexure pivot for aerospace mechanisms. In Proc 10th European Space Mechanisms and Tribology Symposium, Noordwijk.
- Hildebrand, S. 1958. Obliczanie i zachowanie sie w pracy sprzyn krzyzowych. *Pomiary-Automatyka-Kontrola* 11:501–08.

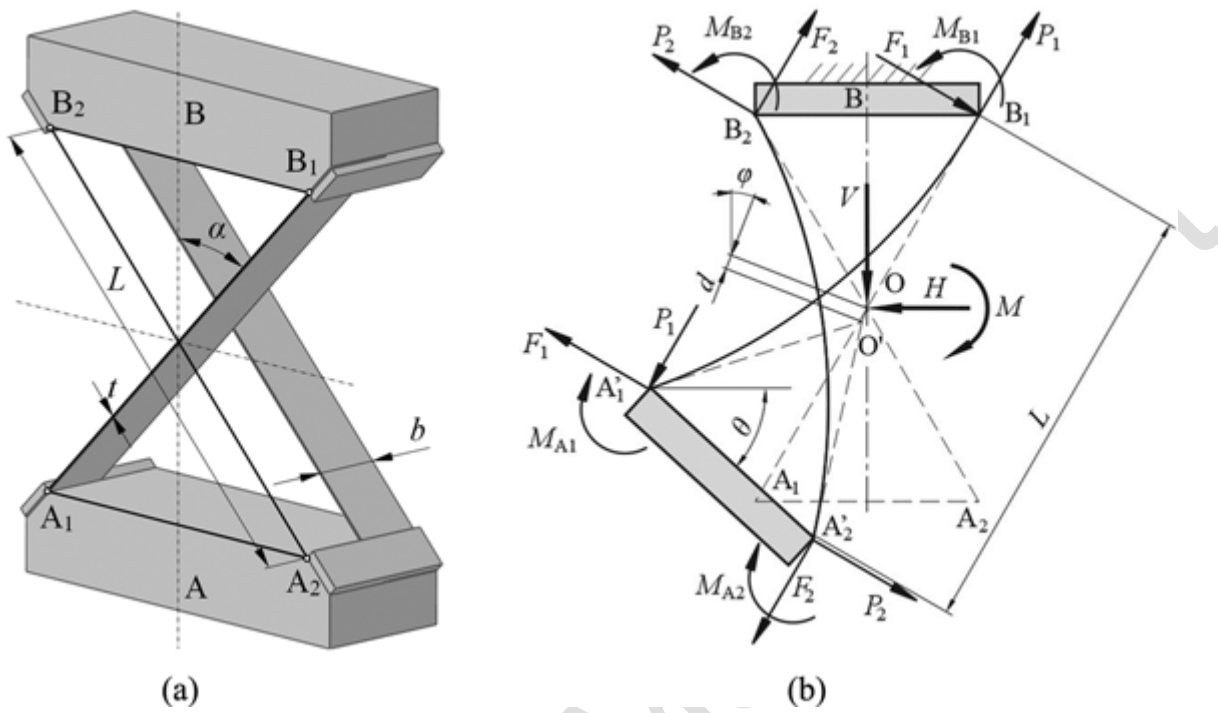
- Hongzhe, Z., and B. Shusheng. 2010. Accuracy characteristics of the generalized cross-spring pivot. *Mechanism and Machine Theory* 45:1434–48. doi:10.1016/j.mechmachtheory.2010.05.004
- Howell, L. L. 2001. *Compliant mechanisms*. New York: Wiley & Sons.
- Ivanov, I., and B. Corves. 2014. Stiffness-oriented design of a flexure hinge-based parallel manipulator. *Mechanics Based Design of Structures and Machines* 42 (3):326–42. doi:10.1080/15397734.2014.899913
- Jensen, B. D., and L. L. Howell. 2002. The modelling of cross-axis flexural pivots. *Mechanism and Machine Theory* 37:461–76. doi:10.1016/s0094-114x(02)00007-1
- Jones, R. V. (1962). Some uses of elasticity in instrument design. *Journal of Scientific Instruments* 39:193–203. doi:10.1088/0950-7671/39/5/303
- Khan, S., and G. K. Ananthasuresh. 2014. A micromachined wide-band in-plane single-axis capacitive accelerometer with a displacement-amplifying compliant mechanism. *Mechanics Based Design of Structures and Machines* 42 (3):355–70. doi:10.1080/15397734.2014.908299
- Lobontiu, N. (2003). *Compliant mechanisms – Design of flexure hinges*. Boca Raton: CRC Press.
- National Physical Laboratory. 1956. *Notes on applied science No. 15*. London: H. M. Stationary Office.
- Nickols, L. W., and H. L. Wunsch. 1951. Design characteristics of cross-spring pivots. *Engineering* 473–76.
- Pavlović, N. D., and T. D. Pavlović. 2013. *Gipki mehanizmi*. Niš: University of Niš.
- Pei, X., J. Yu, G. Zong, and S. Bi. 2010. An effective pseudo-rigid-body method for beam-based compliant mechanisms. *Precision Engineering* 34:634–39. doi:10.1016/j.precisioneng.2009.10.001
- Siddall, G. J. 1970. The design and performance of flexure pivots for instruments. M.Sc. Thesis., Aberdeen, University of Aberdeen.
- Smith, S. T. 2000. *Flexures: Elements of elastic mechanisms*. Amsterdam: Gordon and Breach Science Publishers.
- Smith, S. T., and D. G. Chetwynd. 1992. *Foundations of ultraprecision mechanism design*. Amsterdam: Gordon and Breach Science Publishers.
- Troeger, H. 1962. Considerations in the application of flexural pivots. *Automatic Control* 17 (4):41–46.
- Wittrick, W. H. 1948. The theory of symmetrical crossed flexure pivots. *Australian Journal of Chemistry* 1 (2):121–34. doi:10.1071/ch9480121c
- Wittrick, W. H. 1951. The properties of crossed flexure pivots and the influence of the point at which the strips cross. *The Aeronautical Quarterly* 2:272–92. doi:10.1017/s0001925900000470
- Wuest, W. 1950. Blattfedergelenke für messgeräte. *Feinwerktechnik* 54 (7):167–70.
- Yin, L., and G. K. Ananthasuresh. 2003. Design of distributed compliant mechanisms. *Mechanics Based Design of Structures and Machines* 31 (2):151–79. doi:10.1081/sme-120020289
- Young, W. E. 1944. An investigation of the cross-spring pivot. *Journal of Applied Mechanics* 11:A113–A120.
- Zelenika, S., and F. De Bona. 2002. Analytical and experimental characterisation of high-precision flexural pivots subjected to lateral loads. *Precision Engineering* 26:381–88. doi:10.1016/s0141-6359(02)00149-6

Figure 1. Two most typical design configurations of a symmetrical cross-spring pivot.



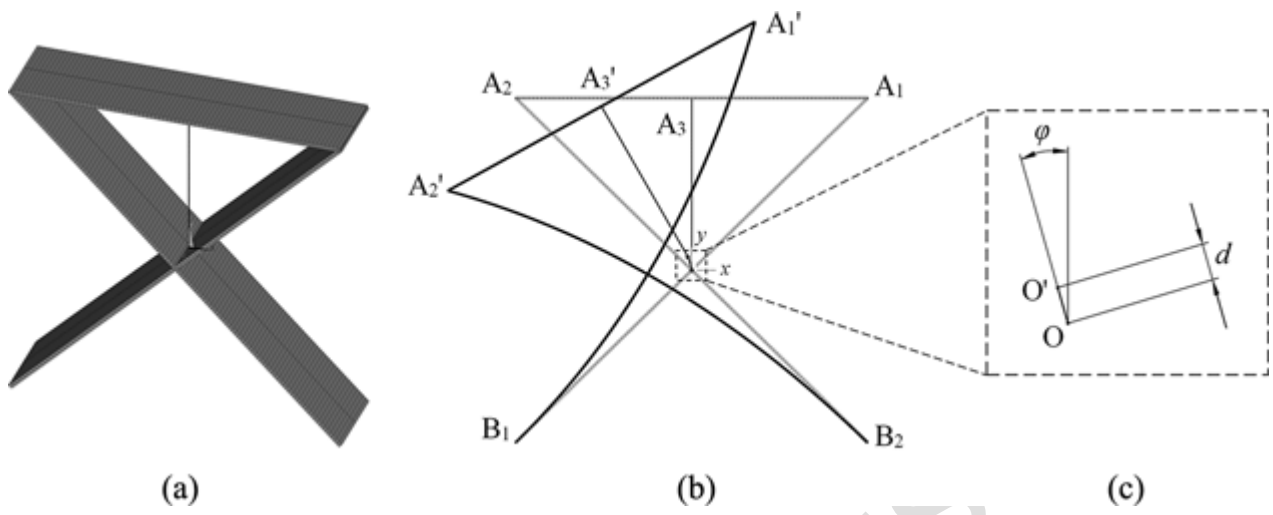
Accepted Manuscript

Figure 2. Parameters of the design of a cross-spring pivot (a) and equilibrium condition in deformed position (b).



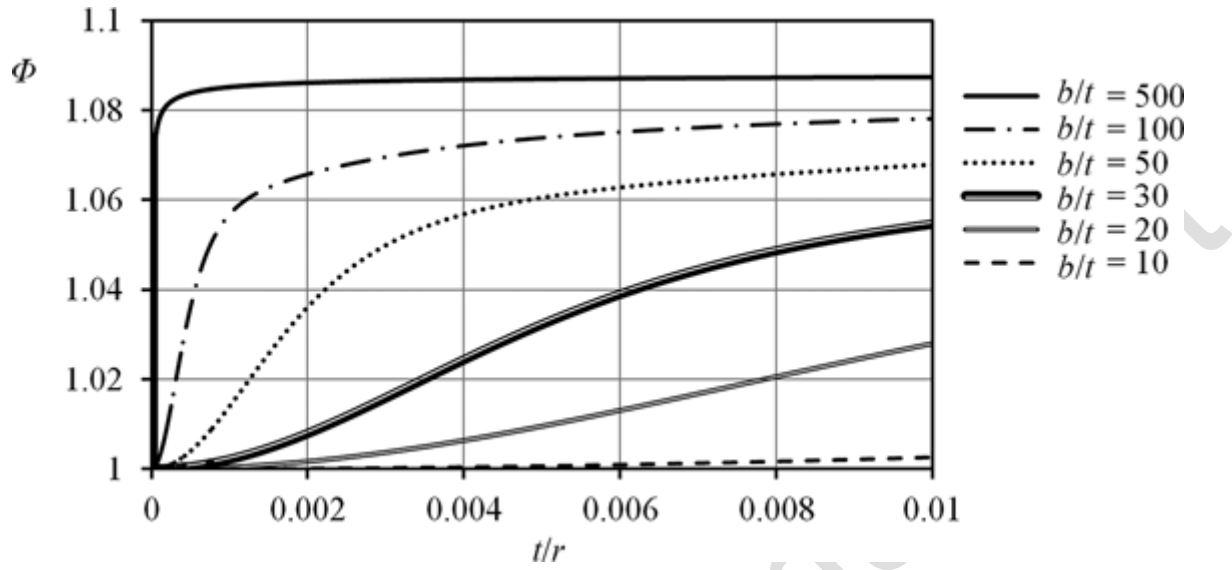
Accepted Manuscript

Figure 3. Finite element model (a), deformed shape of the pivot (b) and its parasitic shift (c).



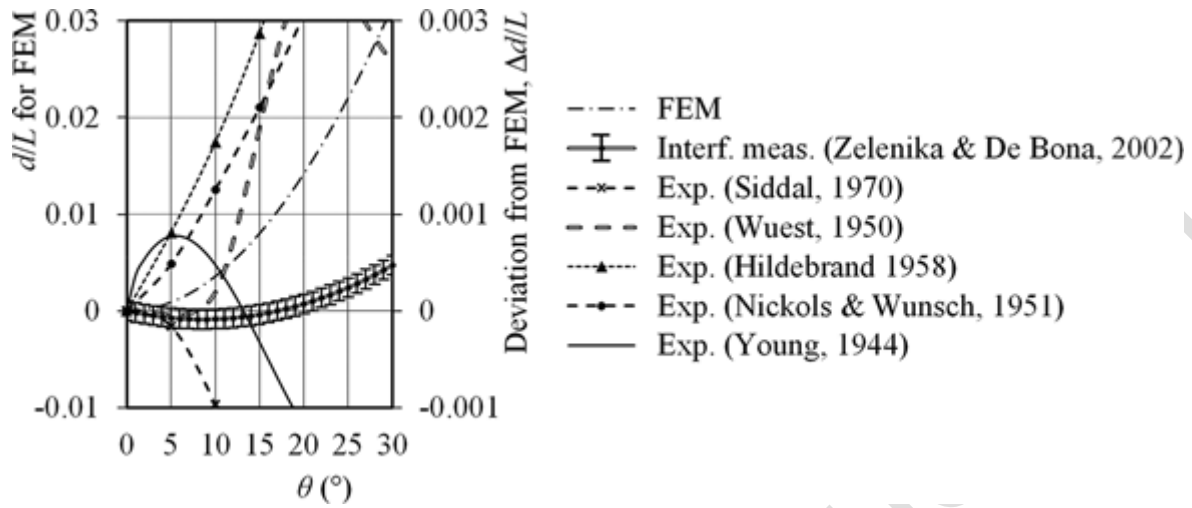
Accepted Manuscript

Figure 4. Dependence of the factor Φ on the normalised curvature and dimension of the leaf springs.



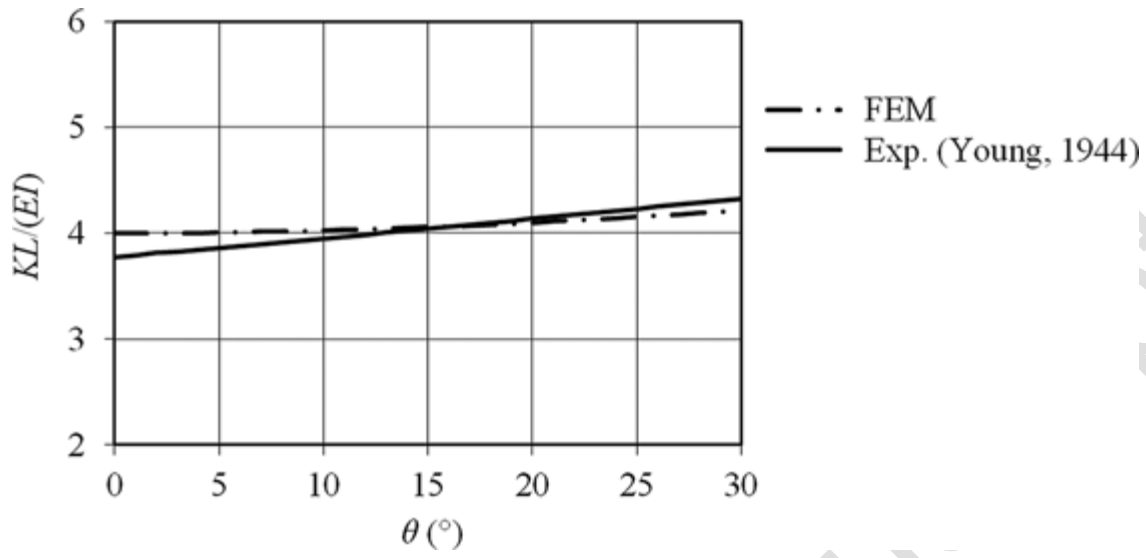
Accepted Manuscript

Figure 5. Differences $\Delta d/L$ of various experimental results with respect to FEA normalized parasitic shift amplitudes.



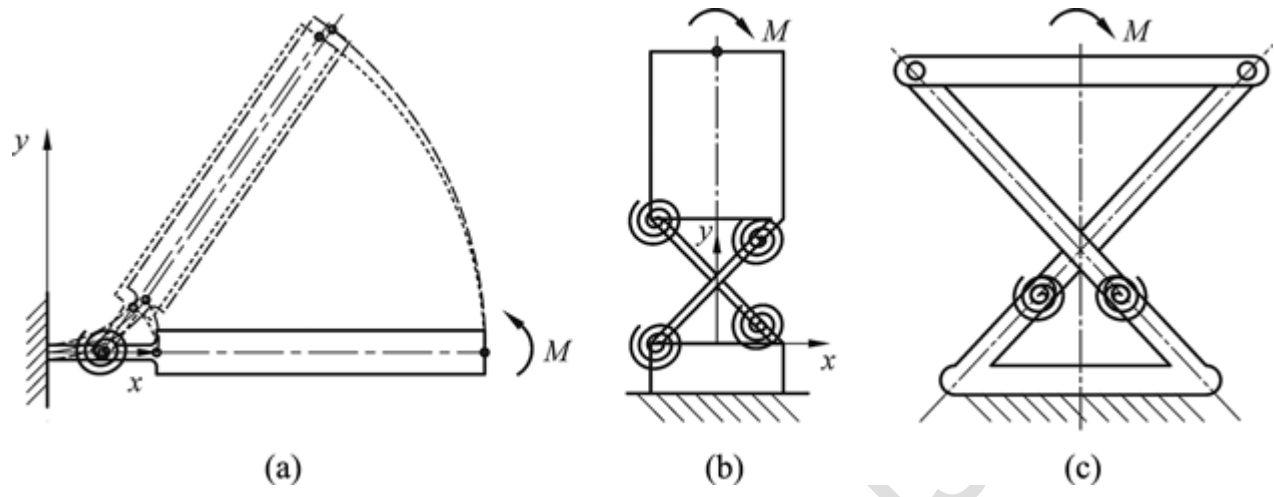
Accepted Manuscript

Figure 6. Rotational stiffness obtained via FEM analysis and measured experimentally.



Accepted Manuscript

Figure 7. PRBM in the ‘pin joint’ (a) and the ‘four bar’ arrangements (Jensen and Howell 2002) (b), as well as in the ‘two rigid bars with two pin joints each’ configuration (Pei et al., 2010) (c).



Accepted Manuscript

Figure 8. Comparison of FEA and results of various modelling tools in terms of normalised parasitic shift amplitudes (a) and couples (b) vs. rotation angle θ .

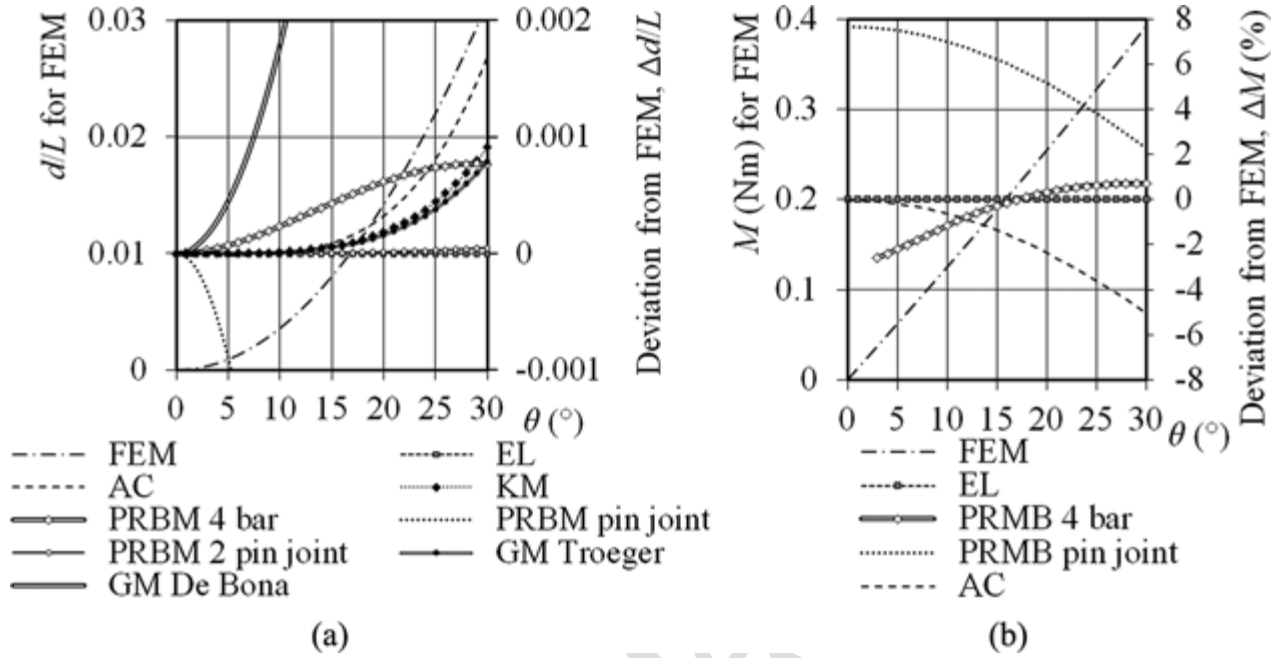


Figure 9. Considered design configurations of cross-spring pivots.

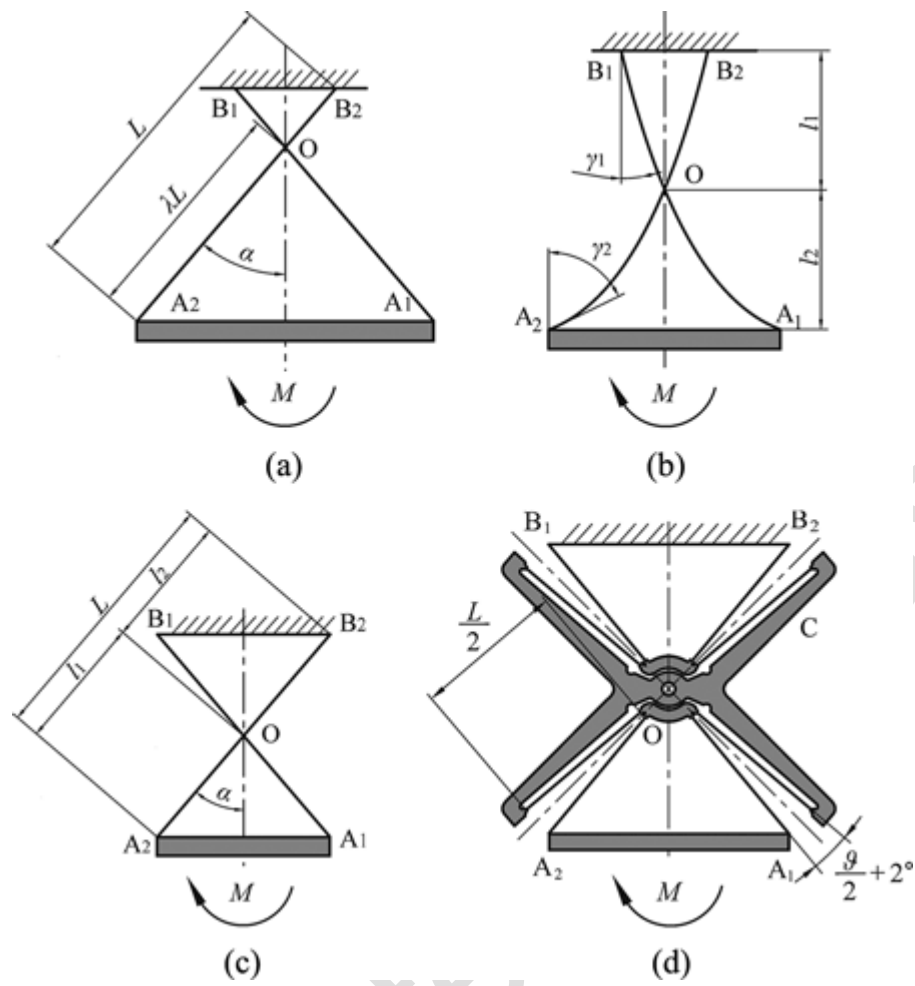
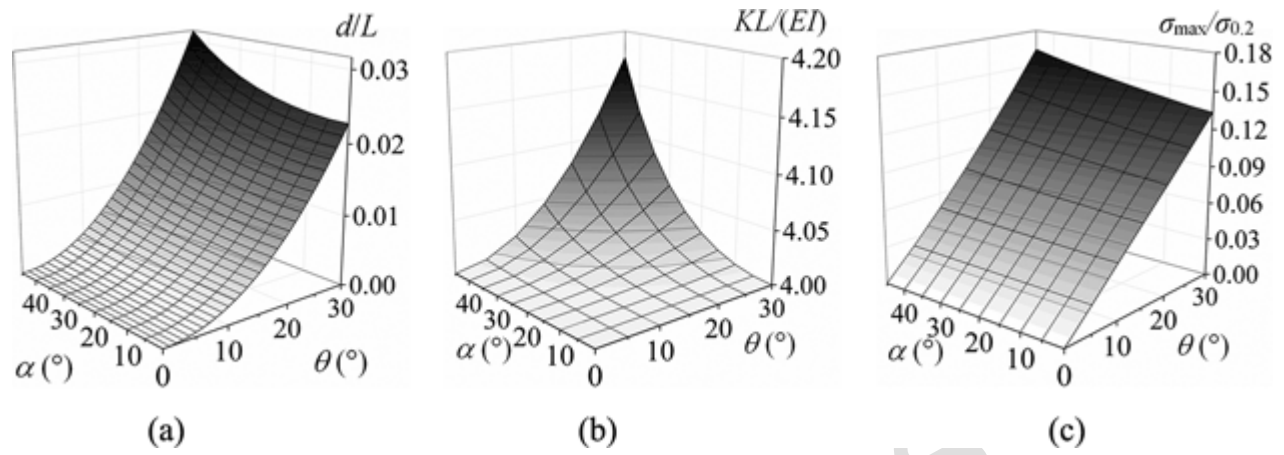
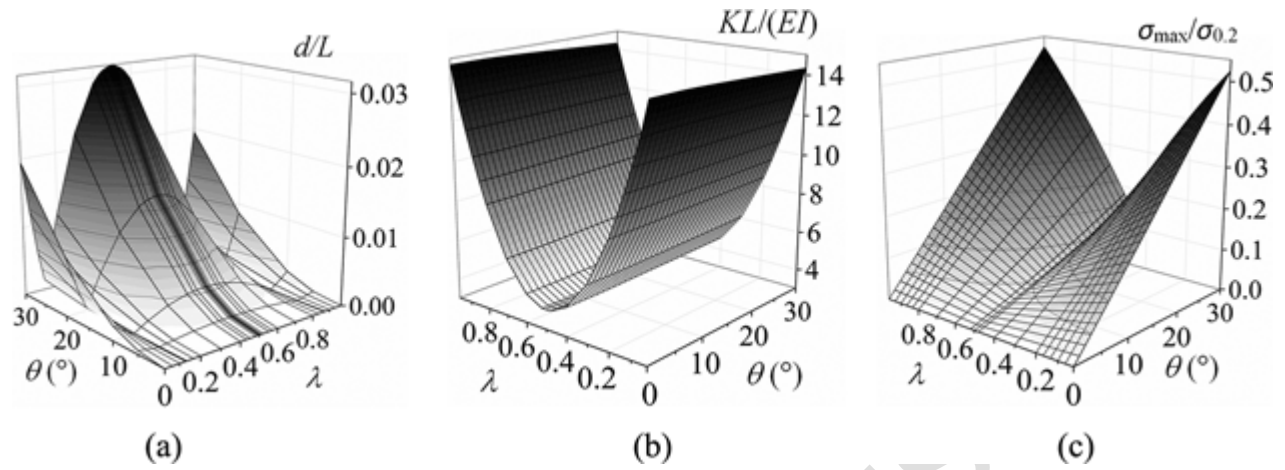


Figure 10. Change of normalised parasitic shift amplitudes (a), normalised rotational stiffness (b) and normalised stresses (c) vs. rotation θ depending on the inclination α of the springs.



Accepted Manuscript

Figure 11. Change of normalised parasitic shift amplitudes (a), normalised rotational stiffness (b) and normalised stresses (c) vs. θ depending on λ for the configuration with $\alpha = 45^\circ$.



Accepted Manuscript

Figure 12. Change of normalised parasitic shift amplitudes (a), normalised rotational stiffness (b) and normalised stresses (c) vs. θ for a monolithic pivot with $\alpha = 15^\circ$ (dashed line), $\alpha = 30^\circ$ (compound line with circular markers) and $\alpha = 45^\circ$ (solid line).

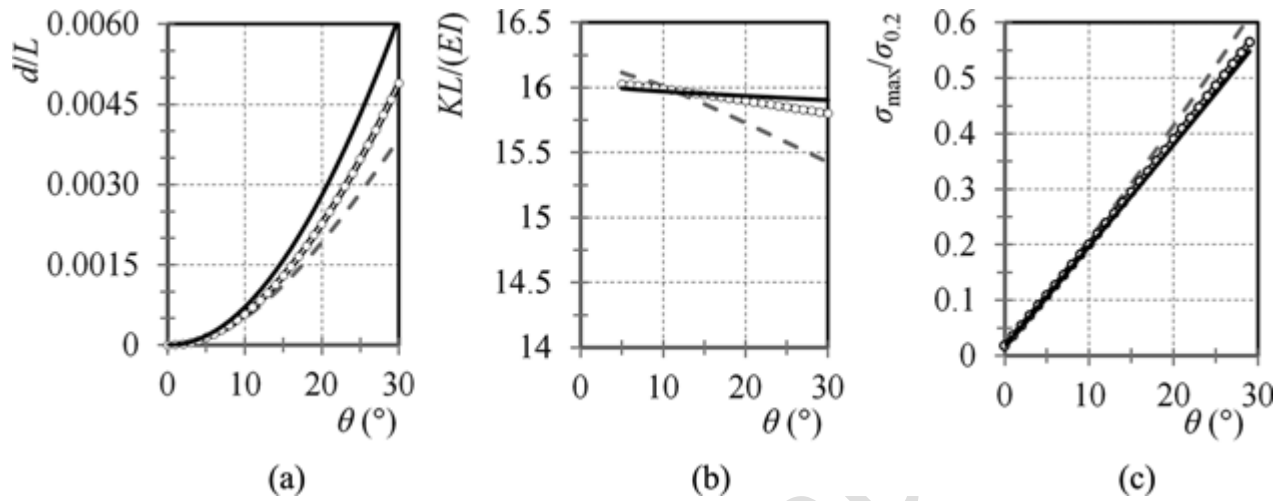
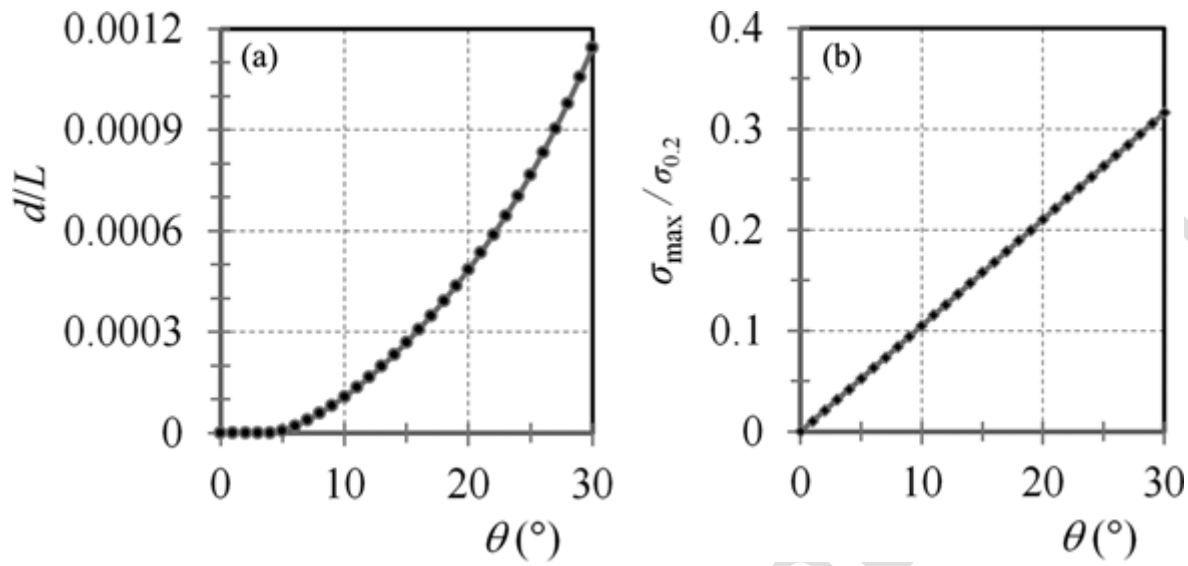


Figure 13. Change of the normalised parasitic shift amplitudes (a) and normalised stresses (b) vs. θ for a “butterfly” pivot configuration.



Accepted Manuscript

Figure 14. Dependence of the normalised rotational stiffness of the pivot on vertical loads for various values of the geometric parameter λ when $\alpha = 45^\circ$.

